ORIGINAL SCIENTIFIC PAPER

CROATICA CHEMICA ACTA

Croat. Chem. Acta **2019**, *92*(3), 403–410
Published online: October 13, 2019
DOI: 10.5562/cca3555

HKD 1926

Kinetic Evaluation of the Charge Migration and H_2O_2 Transport Rates During the Electrocatalytic Reduction of H_2O_2 on Thin Prussian Blue Films

Egon Rešetar, Sandra Čičić, Damir Iveković*

[1] Laboratory for general and inorganic chemistry and electroanalysis, Department of chemistry and biochemistry, Faculty of food technology and biotechnology, University of Zagreb, Pierottijeva 6, HR-10000 Zagreb, Croatia

* Corresponding author's e-mail address: divekov@pbf.hr

RECEIVED: July 24, 2019 * REVISED: October 1, 2019 * ACCEPTED: October 1, 2019

Abstract: Kinetic analysis of the electrocatalytic reduction of H_2O_2 on electrodes modified with thin Prussian blue films was performed and a full set of kinetic parameters governing the rate of the electrocatalytic reaction was determined. Rate constant ($\kappa \cdot k'$) for the catalytic reaction between H_2O_2 and the reduced form of Prussian blue incorporating interstitial Cs^+ and K^+ ions was calculated to be equal to $3.1 \cdot 10^6$ and $2.3 \cdot 10^6$ $cm^3 \cdot mol^{-1}\ s^{-1}$, respectively. The diffusion coefficient of H_2O_2 and the apparent diffusion coefficient of electrons in the reduced form of Prussian blue were found to be $\kappa \cdot D_S(H_2O_2) = 2.6 \cdot 10^{-7}$ cm^2/s and $D_e = 2.8 \cdot 10^{-12}$ cm^2/s, respectively.

Keywords: iron(III) hexacyanoferrate(II), Prussian blue, electron transport, H_2O_2 diffusion, electrocatalysis, kinetics.

INTRODUCTION

SINCE the first report on the electrocatalytic reduction of hydrogen peroxide on electrodes modified with thin redox-active films of Prussian blue (PB) by Itaya in 1984,[1] PB has been considered as one of the best non-platinum group metal catalysts for electrochemical reduction of H_2O_2, especially for the applications in electrochemical hydrogen peroxide sensors and biosensors based on oxidase enzymes.[2–5] Chemically, PB is iron(III) hexacyanoferrate(II), a polymeric, non-stoichiometric mixed-valence compound, which composition can vary between two limiting stoichiometries, the so-called "insoluble PB", $Fe^{(III)}_4[Fe^{(II)}(CN)_6]_3$, and "soluble# PB", $MFe^{(III)}[Fe^{(II)}(CN)_6]$, differing in the amount of $[Fe^{(II)}(CN)_6]^{4-}$ vacancies situated at the Fe^{2+} lattice sites and the number of monovalent cations M^+ (typically alkali metal cations or NH_4^+) occupying the interstitial sites of the cubic crystal lattice of PB.[6–8],§ Electrocatalytic activity of PB towards hydrogen peroxide reduction relies on the ability of Fe^{3+} ions in PB to be reversibly reduced to the +2 oxidation state [Eq. (1)], giving the reduced form of PB, iron(II) hexacyanoferrate(II), the so-called Prussian white (PW). In the presence of H_2O_2, PW is rapidly and irreversibly oxidized to PB, which in turn can be electrochemically reduced back to PW, leading to the electrocatalytic cycle described by the reactions:[1]

$$\underset{\text{(PB)}}{MFe^{(III)}[Fe^{(II)}(CN)_6]} + M^+ + e^- \rightleftarrows \underset{\text{(PW)}}{M_2Fe^{(II)}[Fe^{(II)}(CN)_6]} \quad (1)$$

$$M_2Fe^{(II)}[Fe^{(II)}(CN)_6] + \tfrac{1}{2}H_2O_2 \rightarrow MFe^{(III)}[Fe^{(II)}(CN)_6] + M^+ + OH^- \quad (2)$$

in which the stoichiometry of PB is, for simplicity, assumed to correspond to soluble PB. Due to the microporous (zeolitic) nature of PB, electrocatalytic reduction of H_2O_2 on the PB-modified electrodes occurs within the volume of the PB film,[1] making PB a very efficient H_2O_2 reduction catalyst.

Due to the potential application of PB in electrochemical sensors, the majority of research on the electrocatalytic reduction of H_2O_2 on the PB-modified electrodes conducted so far has been focused on optimizing the catalytic performances of PB with an aim to increase the sensitivity of the PB-modified electrodes towards H_2O_2 or to increase their stability.[9–15] Papers dealing with the kinetics of the electrocatalytic reduction of

The designation "soluble" is misleading, because both "soluble" and "insoluble" forms of PB are highly insoluble in water. However, "soluble" PB is prone to peptization in aqueous solutions of low ionic strength, hence the name.

§ Different forms of PB also differ in the amount of H_2O molecules and OH^- ions coordinated to the Fe^{3+} ions located at the lattice sites surrounding the ferrocyanide vacancies.[7,8] For clarity, these ligands are ommited from the formulas given in the text.

H_2O_2 on PB are relatively scarce and limited to evaluation of the rate constant of heterogeneous catalytic reaction between PB and H_2O_2.[1,16–18] Since the rate of the overall electrocatalytic process occurring within the volume of a thin, three-dimensional electrocatalytic film depends not only on the rate of the heterogeneous catalytic reaction but also on the rates of substrate diffusion and charge propagation through the electrocatalytic film,[19,20] the lack of reliable kinetic parameters that determine the electrocatalytic performances of PB significantly reduces the possibilities for rational design of PB-modified electrodes. In this work, we performed a thorough kinetic analysis of the electrocatalytic reduction of H_2O_2 on electrodes modified with thin PB films within the framework of the kinetic model of the mediated heterogeneous electrochemical catalysis on redox-active films developed by Andrieux and Saveant.[19,20] A full set of kinetic parameters governing the rate of the electrocatalytic reduction of H_2O_2 was determined, with an emphasis on determination of the rates of electron propagation and H_2O_2 transport through thin films of PB in its electrocatalytically active reduced form, which have not been, to the best of our knowledge, determined experimentally so far. Kinetic experiments were performed on films of PB containing interstitial Cs^+ ions, for which we recently found to exhibit a better stability at higher concentrations of H_2O_2 than the commonly studied form of PB containing interstitial K^+ ions. This allowed us to perform kinetic measurements within a wide range of H_2O_2 concentrations, which was prerequisite for reaching kinetic situations in which the electrocatalytic reaction is not controlled solely by the rate of the heterogeneous catalytic step, so that the rates of the transport processes occurring in the electrocatalytic film could be studied.

EXPERIMENTAL

Materials and Instrumentation

All chemicals employed in this work were of analytical grade and were used without further purification. Reagent solutions were prepared with ultra-pure water from Millipore Synergy system. Stock solutions of H_2O_2, $c(H_2O_2)$ = 1 mol dm^{-3}, were prepared on daily basis and stored in dark, and were further dilluted (to the final concentration of 0.25 or 2.75 mmol dm^{-3}) just before use.

Voltammetric measurements were carried out using a Voltalab 50 potentiostat/galvanostat (Radiometer, France). Measurements were performed in a three-electrode cell, with a large-area glassy carbon auxiliary electrode and a Hg/Hg_2Cl_2/3.5M KCl reference electrode (E = 0.250 V vs. SHE at 25 °C). Glassy carbon disc electrodes (d = 6 mm) were employed as working electrodes for cyclic voltammetry and rotating disc electrode (RDE) voltammetry. Spectroelectrochemical measurements were carried out using an optical fiber-coupled CCD spectrometer USB4000 (Ocean Optics, USA), in a home-made spectroelectrochemical cell with a transparent indium-dopped tin oxide (ITO) working electrode. Scanning electron microscopy (SEM) was performed on a Jeol JSM-IT200 microscope operating at 5 kV.

Kinetic measurements were performed at 25 ± 1 °C in a thermostated electrochemical cell. All other experiments were conducted at room temperature. Electrochemical experiments were performed in deoxygenated (N_2-purged) solutions.

Preparation of PB-modified Electrodes

Electrodes covered with thin films of PB containing interstitial Cs^+ or K^+ ions (here referred to as CsPB and KPB, respectively) were prepared according to a slightly modified electrodeposition procedure described in Ref. [21]. In brief, a film of "insoluble" PB (containing no interstitial cations) was first deposited on the electrode surface by imposing the current of –25 μA/cm^2 on the electrode immersed in aqueous solution containing 5 mmol dm^{-3} $FeCl_3$, 5 mmol dm^{-3} $K_3[Fe(CN)_6]$, and 10 mmol dm^{-3} HCl. Insertion of alkali metal cations into the structure of PB was performed by cyclic polarization (at 20 mV/s) of the freshly deposited PB film in the potential range between 0.7 (0.55 for K-PB) and –0.2 V in the deoxygenated solution containing 0.1 mol dm^{-3} CsCl (or KCl) and 10 mmol dm^{-3} HCl, until the voltammograms exhibiting a negligible (typically less than 2 percent) variation of the peak current were obtained. Electrode was then thoroughly washed with deionised water and used for kinetic measurements immediately after the washing. Care was taken not to dry PB films between the preparation steps or prior to kinetic measurements.

Thickness of the PB films was calculated from the charge under the reduction peak on the cyclic voltammograms of PB, by assuming that four electrons per unit cell of PB were consumed for complete reduction of PB and using an unit cell constant of a = 1.016 nm.[6]

RESULTS AND DISCUSSION

Morphological and Electrochemical Eharacterization of CsPB Films

Figure 1 shows typical morphology of the galvanostatically deposited PB films studied in this work. The films were composed of densely packed PB nanoparticles and were uniform in thickness. Although the SEM showed that PB films are highly cracked, no evidence of the film porosity was found when the electrodes with freshly deposited PB

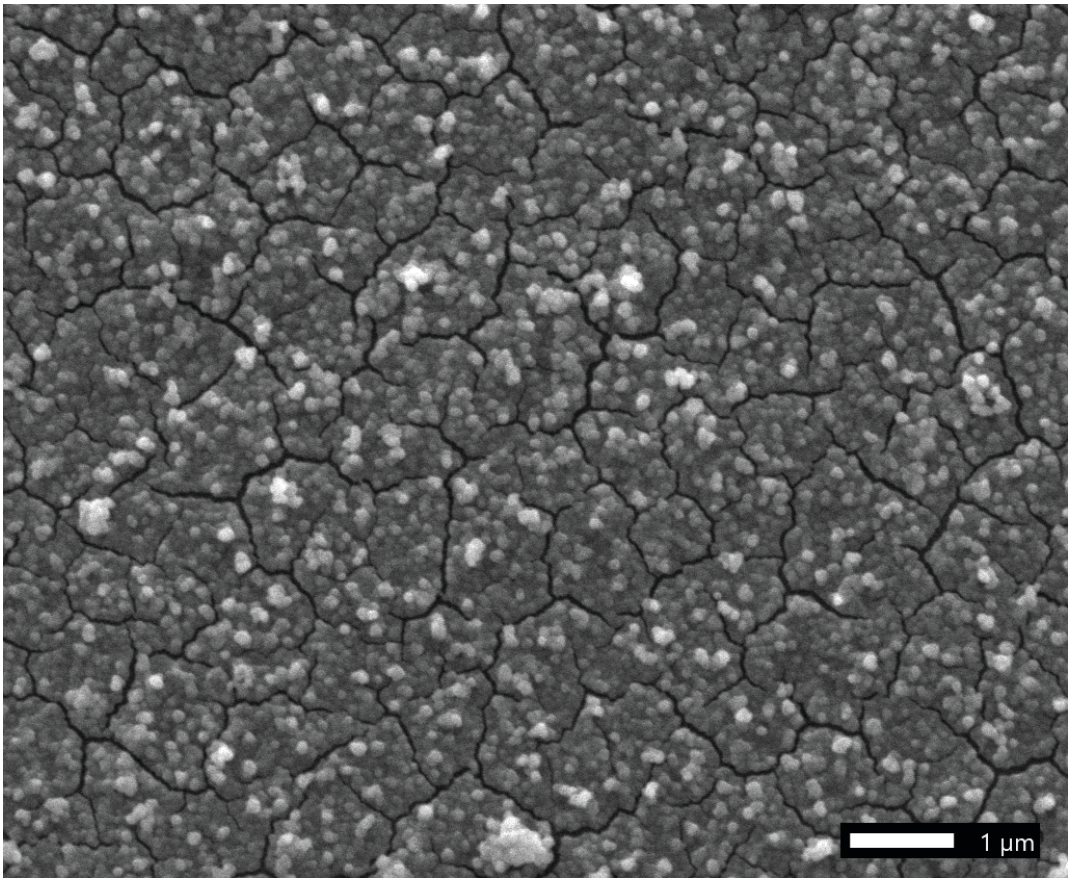

Figure 1. SEM micrograph of the CsPB film deposited on the surface of glassy carbon disc electrode.

films were subjected to potential cycling between 0.7 and –0.2 V in solutions containing 2.5 mmol dm^{-3} Fe^{3+}, 0.1 mol dm^{-3} KCl and 10 mmol dm^{-3} HCl. Only mediated reduction of Fe^{3+} in the potential range corresponding to the reduction of Prussian blue to Prussian white was observed, with no signs of the reduction current at potentials close to the formal potential of the Fe^{3+}/Fe^{2+} redox couple. This strongly indicates that freshly deposited PB film is continuous and uniformly covers the entire electrode surface, and that the cracking of the film probably occurs during its drying and/or dehydration in the high vacuum of the SEM. For this reason, electrochemical measurements were always performed on freshly prepared PB films.

Cyclic voltammogram of the CsPB film recorded in 0.1 mol dm^{-3} CsCl / 10 mmol dm^{-3} HCl solution is shown in Figure 2.a. A pair of broad and asymmetric voltammetric maxima appearing in the potential range between 0.65 and –0.1 V corresponds to the reduction and reoxidation of the nitrogen coordinated Fe^{3+} ions in PB accompanied by insertion and expulsion, respectively, of Cs^+ from the PB film,[22–24] as described by Eq. (1). A close inspection of the voltammogram reveals that both the cathodic and anodic branch of the voltammogram is composed of at least three broad and overlapped peaks appearing at ca. 0.48, 0.28 and 0.09 V, indicating that at least three different redox-active Fe^{3+} centers are present in CsPB. These redox centers can be assigned to the Fe^{3+} ions situated in different coordination environments of the $Fe^{(III)}N_6$, $Fe^{(III)}N_{6-n}(H_2O)_n$ and $Fe^{(III)}N_{6-n}(H_2O)_{n-m}(OH)_m$ type, which simultaneously exist in the crystal lattice of PB containing both the ferrocyanide vacancies and interstitial charge-compensating cations.[7,8] All of these redox centers are electrochemically active and can be fully reduced to the oxidation state of +2, as confirmed by spectroelectrochemical measurements shown in Figure 2.a (gray trace). Voltabsorptogram recorded at 705 nm (a wavelength corresponding to the maximum of absorption of CsPB) clearly shows that the absorbance of the CsPB film disappears at potentials lower than –0.1 V, indicating complete reduction of CsPB to colorless CsPW.

Stationary voltammogram of the reduction of H_2O_2 recorded on the CsPB-modified glassy carbon RDE is shown in Figure2.b. In contrast to the reduction of H_2O_2 on the unmodified glassy carbon electrode, which proceeds with a measurable rate only at potentials lower than ca. –0.12 V, reduction of H_2O_2 on the electrode modified with CsPB

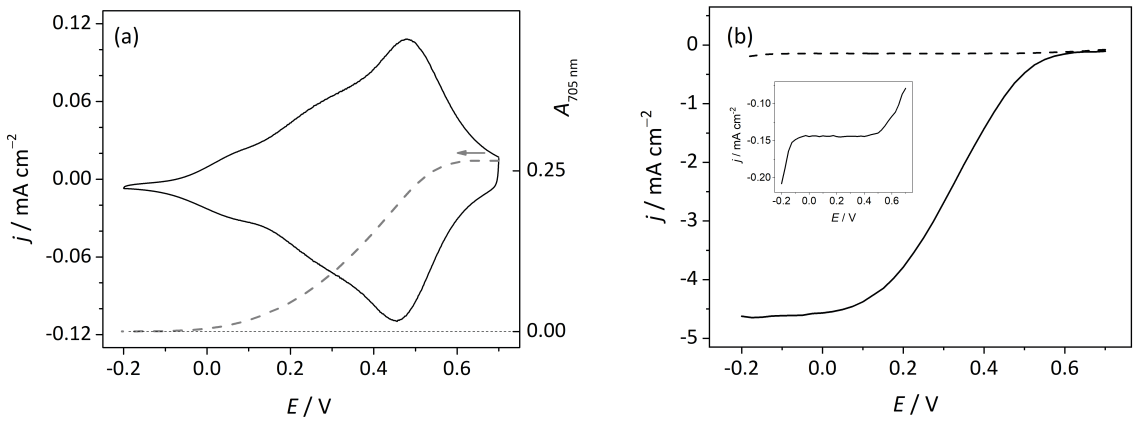

Figure 2. (a) Cyclic voltammogram of the CsPB-modified glassy carbon (GC) electrode (solid line) and the cathodic branch of the voltabsorptogram of the CsPB film deposited on ITO electrode (dashed line), recorded in the 0.1 mol dm^{-3} CsCl / 10 mmol dm^{-3} HCl solution; scan rate: 10 mV/s. **(b)** Stationary RDE voltammogram for the reduction of 2.75 mmol dm^{-3} H_2O_2 on the CsPB-modified GC rotating disc electrode (solid line) and unmodified GC rotating disc electrode (dashed line); supporting electrolyte: 0.1 mol dm^{-3} CsCl / 10 mmol dm^{-3} HCl; electrode rotation rate: 40 rps; Cs-PB film thickness: 56.8 nm. RDE voltammogram for the reduction of H_2O_2 on the unmodified GC electrode is zoomed in the inserted figure.

starts at potentials as high as 0.6 V, demonstrating the high electrocatalytic activity of CsPB towards H_2O_2 reduction. The H_2O_2 reduction current reaches its limiting value at potentials lower than 0 V, coinciding with the potential range in which all of the nitrogen coordinated Fe^{3+} redox-centers in CsPB are reduced (voltabsorptogram in Figure 2.a) and therefore catalytically fully activated. Figure 3.a shows the dependence of the limiting current of H_2O_2 reduction on the electrode rotation rate, recorded on electrodes modified with the CsPB films which thickness varied between 7.5 and 120 nm. As can be seen from the figure, for a given electrode rotation rate, the limiting current increased with the increase of the film thickness, as expected for the electrocatalytic process occurring within the volume of the electrocatalytic film. For a given thickness of the CsPB film, the limiting current increased with the increase of the electrode rotation rate, but the dependence of the limiting current on the square root of the electrode rotation rate was not linear. The latter is a clear indication that the electrochemical process occurring within the CsPB film is only partially controlled by the diffusion of H_2O_2 from the bulk solution to the film surface, i.e. that some other process (or processes) also affects the rate of the electrocatalytic reduction of H_2O_2.

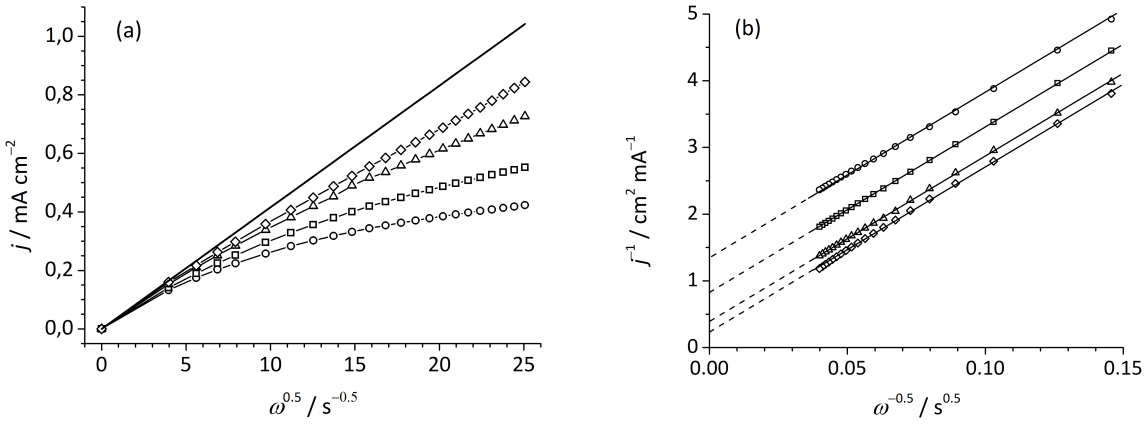

Figure 3. (a) Dependence of the catalytic current for the reduction of 0.25 mmol dm^{-3} H_2O_2, recorded on the glassy carbon rotating disc electrode modified with the CsPB film, on the square root of the electrode rotation rate. CsPB film thickness: (○) 7.5 nm; (□) 14.3 nm; (Δ) 28.5 nm; (◊) 56.8 nm. Diffusion-limited current predicted by the Levich equation is shown by thick solid line. Electrode potential: –0.2 V; supporting electrolyte: 0.1 mol dm^{-3} CsCl / 10 mmol dm^{-3} HCl. **(b)** Koutecky-Levich plots of the data from figure (a).

Adaptation of the Kinetic Model

Generally, an overall rate of the electrocatalytic process occurring within the volume of the redox-active film immobilized on the electrode surface is determined by the relative rates of the following four processes: (*i*) diffusion of the electroactive substance (substrate) from the bulk solution to the film/solution interface, (*ii*) diffusion of the substrate through the film, (*iii*) electron migration through the film and (*iv*) catalytic reaction between the substrate and redox centers in the film. According to the model developed by Andrieux and Saveant for the electrocatalytic reaction occurring under stationary conditions (as in the case of the RDE voltammetry), each of this four processes can be described by the corresponding characteristic current density defined as:[19,20]

substrate diffusion through the solution:

$$j_D = n \cdot F \cdot c \cdot D / \delta \quad (3)$$

substrate diffusion through the film:

$$j_S^* = (1 - j/j_D) \cdot n \cdot F \cdot c \cdot \kappa \cdot D_S / d \quad (4)$$

electron migration through the film:

$$j_E = n \cdot F \cdot \Gamma \cdot D_e / d^2 \quad (5)$$

catalytic reaction:

$$j_k^* = (1 - j/j_D) \cdot n \cdot F \cdot c \cdot \kappa \cdot k \cdot \Gamma \quad (6)$$

in which j (A cm^{-2}) is the measured current density and δ (cm) is the Nernst diffusion layer thickness; n and F (C mol^{-1}) are the number of electrons and the Faraday constant, respectively; c (mol cm^{-3}) is the concentration of the substrate in solution; D, D_S and D_e (cm^2 s^{-1}) are the diffusion coefficient of the substrate in solution, diffusion coefficient of the substrate in the film and apparent diffusion coefficient of electrons in the film, respectively; Γ (mol cm^{-2}) is the surface concentration of the catalytic redox centers, k (cm^3 mol^{-1} s^{-1}) is the catalytic rate constant, κ is the distribution coefficient of the substrate between the film and solution and d (cm) is the film thickness. Andrieux and Saveant showed that the kinetics of the overall electrocatalytic process depends on the values of two dimensionless parameters, j_E/j_k^* and j_S^*/j_k^*, which can be varied by changing the experimental variables such as the concentration of substrate, thickness of the electrocatalytic film and the electrode rotation rate. With a proper choice of the experimental variables, electrocatalytic process can be forced to fall into some of the limiting kinetic cases, for which the kinetic parameters can be readily determined from the values of characteristic currents derived from kinetic analysis.

Described kinetic model can be readily extended to electrocatalytic redox films consisting of more than one type of the catalytic redox centers. Under the assumption that the catalytic redox centers behave independently, a partial catalytic current density ($j_{k,i}^*$) defined as:

$$j_{k,i}^* = (1 - j/j_D) \cdot n \cdot F \cdot c \cdot \kappa \cdot k_i \cdot x_i \cdot \Gamma \quad (7)$$

can be assigned to each particular redox center type, which molar fraction in the electrocatalytic film is x_i. Characteristic catalytic current then can be expressed as:

$$j_k^* = \sum j_{k,i}^* = (1 - j/j_D) \cdot n \cdot F \cdot c \cdot \kappa \cdot \Gamma \cdot \sum (k_i \cdot x_i) \quad (8)$$

By introducing the overall catalytic constant defined as:

$$k' = \sum (k_i \cdot x_i) \quad (9)$$

relation (8) reduces to the form analogous to equation (6):

$$j_k^* = (1 - j/j_D) \cdot n \cdot F \cdot c \cdot \kappa \cdot k' \cdot \Gamma \quad (10)$$

Therefore, by replacing Eq. (6) with Eq. (10), kinetic model developed by Andrieux and Saveant can be employed to kinetic analysis of electrocatalytic redox films containing an arbitrary number of the catalytic redox centers of the different type.

Kinetic Analysis

Figure 3.b shows the Koutecky-Levich plots for the data shown in Figure 3.a. Linear plots of the reciprocal current densities on the $1/\omega^{0.5}$ were achieved for all film thicknesses, with a non-zero intercepts, confirming that the electrocatalytic reduction of H_2O_2 is under mixed control. From the slope of the Koutecky-Levich plots shown in Figure 3.b (24.7 ± 0.4 cm^2 s$^{1/2}$ mA^{-1}), the value of the diffusion coefficient of H_2O_2 in solution equal to (1.58 ± 0.03)·10^{-5} cm^2/s was calculated, which is in excellent agreement with the published value of 1.59·10^{-5} cm^2/s at pH 2.0.[25] According to the model developed by Andrieux and Saveant, linear Koutecky-Levich plots can be obtained for a number of kinetic cases. In order to resolve which kinetic cases correspond to the data shown in Figure 3, current densities shown in Figure 3.a were normalized by dividing with $(1-j/j_D)$ and plotted against $(1-j/j_D)$ (Figure 4). Such a plot gives constant values of $j/(1-j/j_D)$ only in the following two kinetic cases: (*i*) pure kinetic control of the electrocatalytic reaction ("R case" according to the designations introduced by Andrieux and Saveant[19,20]) and (*ii*) mixed control, in which both the rate of the substrate diffusion through the film and the rate of the catalytic reaction limit the rate of the overall electrocatalytic process, with the rate of electron transport being much higher than the rates of the other processes (R+S case). As can be seen from Figure 4, a constant values of $j/(1-j/j_D)$ were obtained only for the thinnest CsPB film (d = 7.5 nm), and for this film $j/(1-j/j_D)$ coincides with the Koutecky-Levich intercept. For all other film thicknesses, $j/(1-j/j_D)$ tends to constant values only at high electrode rotation rates, but the limiting values of $j/(1-j/j_D)$ are significantly

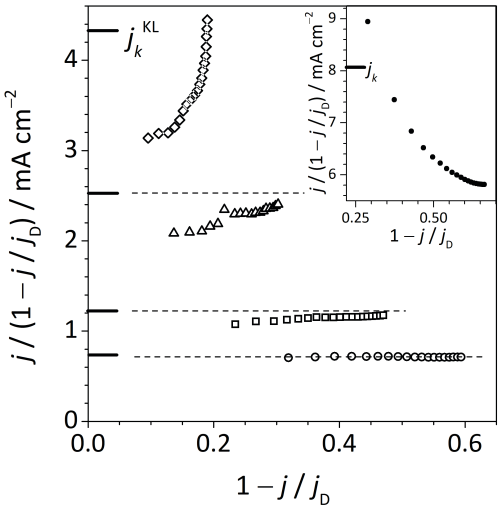

Figure 4. Analysis of the data from Figure 3.a according to the rate laws for the electrocatalytic reaction under pure kinetic control (kinetic "R case"), $j=(1-j/j_D)\cdot j_k$, and electrocatalytic reaction controlled both by the rate of H_2O_2 diffusion through the catalytic film and the rate of the catalytic reaction (kinetic "R+S case"), $j=(1-j/j_D)\cdot(j_k\cdot j_s)^{0.5}\cdot\tanh(j_k/j_s)^{0.5}$.[20] Data markers are identical as in Figure 3.a. Thick black lines next to an *y*-axis and dashed horizontal lines indicate the values of the corresponding Koutecky-Levich intercepts (Figure 3.b). Inset shows the data obtained for the electrocatalytic reduction of 2.75 mmol dm^{-3} H_2O_2 on the rotating disc electrode modified with the 7.5 nm thick CsPB film (other experimental conditions identical as in Figure 3).

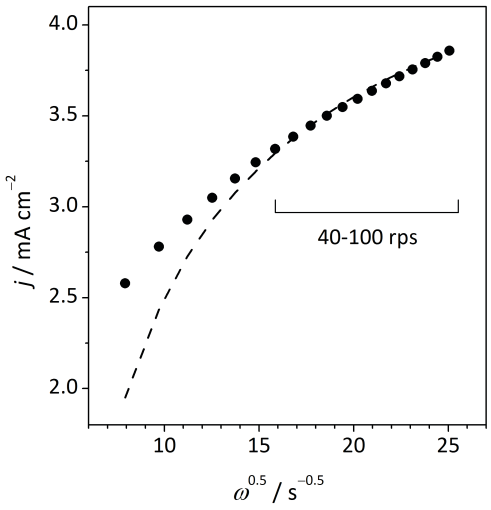

Figure 5. Dependence of the catalytic current for the reduction of 2.75 mmol dm^{-3} H_2O_2, recorded on the glassy carbon rotating disc electrode modified with the 7.5 nm thick CsPB film, on the square root of the electrode rotation rate. Dashed line shows a best fit of the rate law for the electrocatalytic reaction controlled both by the rate of the electron propagation through the catalytic film and the rate of the catalytic reaction (kinetic "R+E case", Eq. (11)) to the points corresponding to the catalytic currents measured at electrode rotation rates greater than 40 rps.

lower than the corresponding Koutecky-Levich intercepts. The latter is inconsistent with the predictions of the model for the kinetic R+S case.[20] In addition, fitting the data in Figure 4 by using the values of D_s and k' calculated under the assumption that the kinetics of the H_2O_2 reduction on the electrode modified with the 7.5 nm CsPB film can be modeled by the kinetic R+S case gave inconsistent results. This leads to the conclusion that the electrocatalytic reduction of H_2O_2 on the electrode modified with the 7.5 nm thick film of CsPB corresponds to the kinetic R case, for which the value of $j/(1-j/j_D)$ is equal to j_k.[20] From the value of $j/(1-j/j_D)$ determined from Figure 4 (0.71 mA/cm^2) and by using Eq. (10), the value of $\kappa\cdot k'$ equal to $3.1\cdot10^6$ cm^3 mol^{-1} s^{-1} was calculated for the CsPB film.

According to the kinetic zone diagram given by Andrieux and Saveant (Figure 1 in Ref. [20] also see Figure 7 here), by increasing the concentration of substrate and by increasing the electrode rotation rate, the electrocatalytic reaction initially falling within the boundaries of the kinetic R case can be pushed towards the R+E case, in which the overall rate of the electrocatalytic reaction depends both on the rate of the catalytic reaction and the rate of the charge propagation through the film.[19,20] For this reason we measured the limiting current of the H_2O_2 reduction on the electrode modified with the 7.5 nm thick CsPB film in solution containing approximately one order of the magnitude higher concentration of H_2O_2 than in the case of the data shown in Figure 3. The measured limiting currents and the currents normalized by $(1-j/j_D)$ are shown in Figure 5 and as inset in Figure 4., respectively. For the kinetic R+E case, limiting current is given by:[20]

$$j = (j_k^*\cdot j_E)^{1/2}\cdot\tanh(j_k^*/j_E)^{1/2} \qquad (11)$$

A best fit of Eq. (11) to the points in Figure 5 corresponding to the electrode rotation rates of 40 rps and higher is shown by the dashed line. From the fit, the value of j_E equal to 4.59 mA/cm^2 was obtained, from which the value of $D_e = 2.8\cdot10^{-12}$ cm^2/s was calculated by using Eq. (5).

In order to determine the value of the remaining kinetic parameter, $\kappa\cdot D_S(H_2O_2)$, we performed a trial-and-error fit of the data from Figure 3.a by using the calculated values of the parameters $\kappa\cdot k'$ and D_e, and varying the parameter $\kappa\cdot D_S$. We found that the H_2O_2 reduction currents measured on the electrode modified with the 14.3 nm thick film of CsPB at high electrode rotation rates can be fitted with an accuracy of better than 90 % if modeled as the R+E case (Figure 6). This indicates that the corresponding points in the kinetic zone diagram should be located close to the

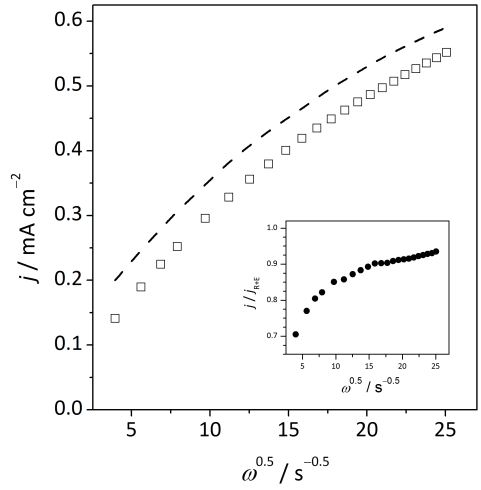

Figure 6. Dependence of the catalytic current for the reduction of 0.25 mmol dm^{-3} H_2O_2, recorded on the glassy carbon rotating disc electrode modified with the 14.3 nm thick CsPB film, on the square root of the electrode rotation rate. Dashed line shows a best fit of the rate law for the electrocatalytic reaction controlled both by the rate of the electron propagation through the catalytic film and the rate of the catalytic reaction (kinetic "R+E case", Eq. (11)) to the measured catalytic currents. Ratio of the measured and fitted current is shown in inset.

boundary of the R+E kinetic zone, which lies at $\log(j_S/j_k)^{0.5} \approx 0.4$.[20] From this condition, the value of j_S was estimated to be approximately 8.64 mA/cm^2, from which the value of $\kappa \cdot D_S$ equal to $2.6 \cdot 10^{-7}$ cm^2/s was calculated by using Eq. (4).

By using the values of the kinetic parameters $\kappa \cdot k'$, D_e and $\kappa \cdot D_S$, the positions of the points corresponding to the measured currents shown in Figures 3.a and 5 in the kinetic zone diagram were finally calculated. The result is shown in Figure 7. Validity of the obtained kinetic parameters was tested by plotting in the kinetic zone diagram also the points corresponding to the H_2O_2 reduction currents measured on the electrode modified with the CsPB film thicker than the films employed for kinetic analysis and the electrodes modified with the KPB films. For the latter, the value of the catalytic rate constant $\kappa \cdot k'$ was determined to be equal to $2.3 \cdot 10^6$ cm^3 mol^{-1} s^{-1} by employing an identical procedure as described for the CsPB film. From the positions of the test points in the kinetic zone diagram (Figure 7), a pure R case was predicted for the electrode modified with the 8.3 nm thick KPB film, and the general case for the test electrodes modified with thicker CsPB (118 nm) and KPB (63 nm) films. Plots of the normalized current $j/(1-j/j_D)$ vs. $(1-j/j_D)$ for the test data were found to be consistent with such predictions (inset in Figure 7).

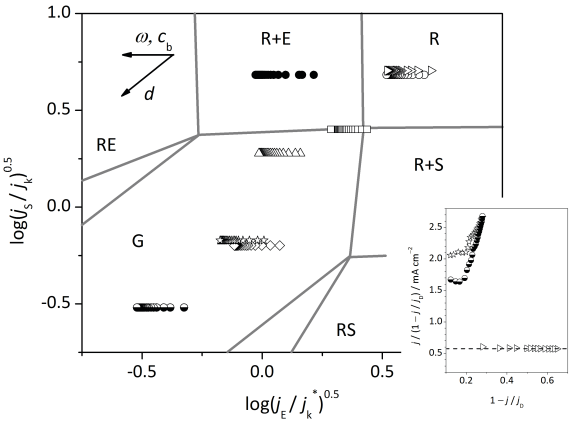

Figure 7. Kinetic zone diagram for the data shown in Figure 3.a and Figure 5. Included are also the points corresponding to the catalytic currents measured for the reduction of 0.25 mmol dm^{-3} H_2O_2 on electrodes modified with the 8.3 nm thick KPB film (▷), 63 nm thick KPB film (☆) and 118 nm thick CsPB film (◒) (referred as "test data" in the text). Other data markers are identical as in Figure 3.a and Figure 5.
The effect of the variation of the experimental parameters (concentration of H_2O_2, c_b; electrode rotation rate, ω; film thickness, d) on the kinetic control of the overall electrocatalytic reaction is indicated by arrows located in the upper left corner of the kinetic zone diagram. Designations of the kinetic zones (R, R+E etc.) are identical as in Ref. [20]. Boundaries between the kinetic zones are according to the Figure 1 in Ref. [20].
Inset shows the analysis of the test data according to the rate law for the electrocatalytic reaction under pure kinetic control (kinetic "R case"), $j = (1-j/j_D) \cdot j_k$.

CONCLUSION

A thorough kinetic analysis of the electrocatalytic reduction of H_2O_2 on electrodes modified with thin films of PB within the framework of the kinetic model of the mediated heterogeneous electrochemical catalysis on redox-active films developed by Andrieux and Saveant allowed us to calculate the values of all three kinetic parameters that determine the rate of the overall electrocatalytic process: the overall rate constant of the catalytic reaction ($\kappa \cdot k'$), the diffusion coefficient of H_2O_2 in the reduced form of PB ($\kappa \cdot D_S$) and the apparent electron diffusion coefficient in the reduced form of PB (D_e). The following values of the kinetic parameters were determined: $\kappa \cdot k'$(CsPB) = $3.1 \cdot 10^6$ cm^3 mol^{-1} s^{-1}, $\kappa \cdot k'$(KPB) = $2.3 \cdot 10^6$ cm^3 mol^{-1} s^{-1}, $D_e = 2.8 \cdot 10^{-12}$ cm^2/s and $\kappa \cdot D_S = 2.6 \cdot 10^{-7}$ cm^2/s. These kinetic parameters allow the detailed kinetic analysis of the PB films to be performed and pave the way to the rational design of PB-based catalytic electrodes in terms of maximizing their catalytic efficiency for H_2O_2 reduction.

REFERENCES

[1] J. C. Hidalgo-Acosta, M. A. Mendez, M. D. Scanlon, H. Vrubel, V. Amstutz, W. Adamiak, M. Opallo, H. H. Girault, *Chem. Sci.***2015**, *6*, 1761–1769. https://doi.org/10.1039/C4SC02196G

[2] R. Garjonyt, A. Malinauskas, *Sensors Actuators B* **1998**, *46*, 236–241. https://doi.org/10.1016/S0925-4005(98)00123-3

[3] M. O. O'Halloran, M.Pravda, G. G. Guilbault, *Talanta* **2001**, *55*, 605–611. https://doi.org/10.1016/S0039-9140(01)00469-6

[4] F. Ricci, G. Palleschi, *Biosensors Bioelectronics* **2005**, *21*, 389–407. https://doi.org/10.1016/j.bios.2004.12.001

[5] B. Kong, C. Selomulya, G. Zheng, D. Zhao, *Chem. Soc. Rev.* **2015**, *44*, 7997–8018. https://doi.org/10.1039/C5CS00397K

[6] H. J. Buser, D. Schwarzenbach, W. Petter, A. Ludi, *Inorg. Chem.* **1977**, *16*, 2704–2710. https://doi.org/10.1021/ic50177a008

[7] P. R. Bueno, F. F. Ferreira, D. Gimenez-Romero, G. O. Setti, R. C. Faria, C. Gabrielli, H. Perrot, J. J. Garcia-Jareno, F. Vicente, *J. Phys. Chem. C* **2008**, *112*, 13264–13271. https://doi.org/10.1021/jp802070f

[8] L. Samain, F. Grandjean, G. J. Long, P. Marinetto, P. Bordet, D. Strivay, *J. Phys. Chem. C*, **2013**, *117*, 9693–9712. https://doi.org/10.1021/jp3111327

[9] F. Ricci, A. Amine, G. Palleschi, D. Moscone, *Biosensors Bioelectronics*, **2003**, *18*, 165–174. https://doi.org/10.1016/S0956-5663(02)00169-0

[10] J. Li, J.-D. Qiu, J.-J. Xu, H.-Y. Chen, X.-H. Xia, *Adv Funct. Mater.* **2007**, *17*, 1574–1580. https://doi.org/10.1002/adfm.200600033

[11] Y. Liu, Z. Chu, W. Jin, *Electrochem. Comm.* **2009**, *11*, 484–487. https://doi.org/10.1016/j.elecom.2008.12.029

[12] Y. Zhang, Z. Chu, L. Shi, W. Jin, *Electrochim. Acta* **2011**, *56*, 8163–8167. https://doi.org/10.1016/j.electacta.2011.05.134

[13] D. Iveković, H. Vlašić Trbić, R. Peter, M. Petravić, M. Čeh, B. Pihlar, *Electrochim. Acta* **2012**, *78*, 452–458. https://doi.org/10.1016/j.electacta.2012.06.027

[14] D. G. B. Limachi, V. R. Goncales, E. P. Cintra, S. I. Cordoba de Torresi, *Electrochim. Acta* **2013**, *110*, 459–464. https://doi.org/10.1016/j.electacta.2013.03.022

[15] S. Cinti, F. Arduini, G. Vellucci, I. Cacciotti, F. Nanni, D. Moscone, *Electrochem. Comm.* **2014**, *47*, 63–66. https://doi.org/10.1016/j.elecom.2014.07.018

[16] A. A. Karyakin, E. E: Karyakina, L. Gorton, *J. Electroanal. Chem.***1998**, *456*, 97–104. https://doi.org/10.1016/S0022-0728(98)00202-2

[17] R. Araminaite, R. Garjonyte, A. Malinauskas, *J. Solid State Electrochem.* **2010**, *14*, 149–155. https://doi.org/10.1007/s10008-009-0802-9

[18] D. Iveković, A. Gajović, M. Čeh, B. Pihlar, *Electroanalysis* **2010,** *22*, 2202–2210. https://doi.org/10.1002/elan.200900622

[19] C. P. Andrieux, J. M. Dumas-Bouchiat, J. M. Saveant, *J. Electroanal. Chem.* **1982**, *131*, 1–35. https://doi.org/10.1016/0022-0728(82)87059-9

[20] C. P. Andrieux, J. M. Dumas-Bouchiat, J. M. Saveant, *J. Electroanal. Chem.* **1984**, *169*, 9–21. https://doi.org/10.1016/0022-0728(84)80069-8

[21] C. A. Lundgren, R. W. Murray, *Inorg. Chem.* **1988**, *27*, 933–939. https://doi.org/10.1021/ic00278a036

[22] K. Itaya, T. Ataka, S. Toshima, *J. Am. Chem. Soc.* **1982**, *104*, 4767–4772. https://doi.org/10.1021/ja00382a006

[23] J. J. Garcia-Jareno, J. Navarro-Laboulais, A. Sanmatias, F. Vicente, *Electrochim. Acta* **1998**, *43*, 1045–1052. https://doi.org/10.1016/S0013-4686(97)00270-3

[24] B. J. Feldman, O. R. Melroy, *J. Electroanal. Chem.* **1987**, *234*, 213–227. https://doi.org/10.1016/0022-0728(87)80173-0

[25] V. G. Prabhu, L. R. Zarapkar, R. G. Dhaneshwar, *Electrochim. Acta* **1981**, *26*, 725–729. https://doi.org/10.1016/0013-4686(81)90029-3

B. J. Feldman, R. W. Murray, *Inorg. Chem.* **1987**, *26*, 1702–1708. https://doi.org/10.1021/ic00258a014